We are IntechOpen,
the world's leading publisher of
Open Access books
Built by scientists, for scientists

4,800
Open access books available

122,000
International authors and editors

135M
Downloads

Our authors are among the

154
Countries delivered to

TOP 1%
most cited scientists

12.2%
Contributors from top 500 universities

BOOK CITATION INDEX INDEXED

CLARIVATE ANALYTICS

WEB OF SCIENCE™

Selection of our books indexed in the Book Citation Index
in Web of Science™ Core Collection (BKCI)

Interested in publishing with us?
Contact book.department@intechopen.com

Numbers displayed above are based on latest data collected.
For more information visit www.intechopen.com

4

In-situ Monitoring of SCC of Alloy 600 SG Tubing in PWR using EN Analysis

Sung-Woo Kim, Hong-Pyo Kim, Seong-Sik Hwang and Dong-Jin Kim
Korea Atomic Energy Research Institute
Republic of Korea

1. Introduction

Nickel based alloys such as Alloy 600 and 690 have been used as the steam generator (SG) tubing materials in a pressurized water reactor (PWR) due to their high corrosion resistance. However, many types of corrosion have occurred in highly caustic environments containing some oxidizing impurities, especially in SG sludge piles, because the highly caustic conditions can be developed in the heated crevices of PWR SG's (Jacko, 1990). Among those impurities, Pb is well known to assist in stress corrosion cracking (SCC) of the SG tubing in the caustic environments (Sakai et al., 1990). Many authors reported on the cracking modes of SCC in Pb-contaminated solutions and the role of Pb on the passive films formed on nickel-based alloys to explain the mechanism of SCC (Hwang et al., 1997; Hwang et al., 1999; Kim et al., 2007; Kim et al., 2008).

Recently, there was an approach to investigate the mechanism by distinguishing between the initiation and propagation stages of Pb-assisted SCC using an electrochemical noise (EN) technique (Kim & Kim, 2009). The EN is defined as a fluctuation of the electrochemical potential or current which is observed experimentally to be associated with localized corrosion processes (Cottis et al., 2001; Stewart et al., 1992). From the analyses of the EN parameters such as the frequency of events, the average charge of events, the noise resistance (Al-Mazeedi & Cottis, 2004; Cottis, 2001; Sanchez-Amyay et al., 2005), and the mean free time-to-failure (Kim & Kim, 2009; Na & Pyun, 2007, Na et al., 20007a, Na et al., 2007b), various types of localized corrosion are distinguishable from each other. Therefore, the EN monitoring technique has become a useful tool for characterizing such localized corrosions as pitting corrosion, crevice corrosion and SCC.

This work is aimed to analyze the EN generated during Pb-assisted SCC of Alloy 600 at high temperature. The EN was measured from C-ring specimens in the highly caustic solution containing oxidizing impurities in two different ways: in a potentiostatic controlled current noise (PCCN) mode, the electrochemical current noise (ECN) was measured from the stressed C-ring specimen by applying an anodic potential. In an uncorrelated three electrode current and potential noise (UCPN) mode, the electrochemical potential noise (EPN) and the ECN were measured simultaneously from the stressed C-ring specimen. Changes in an amplitude and time interval of the ECN and EPN, and variations in power spectral density of the ECN and EPN were analyzed in terms of the initiation and propagation of Pb-assisted SCC of nickel-based alloys in the highly caustic solutions at high temperature.

2. Experimental

2.1 Preparation of C-ring specimens

Alloy 600 SG tubing (Valinox Heat No. NX8527) with 22.23 mm outer diameter (OD), 1.27 mm thickness was used for this work. The chemical composition of the materials is given in Table 1. The tubing was pilgered by the manufacturer, and heat treated in our laboratory at 920 °C for 15 min in an Ar-filled quartz capsule in a furnace, followed by water quenching, to simulate low-temperature mill-annealing (LTMA). The C-ring specimens were fabricated from the Alloy 600 SG tubing in accordance with the ASTM G38 standard. The OD surface of the specimens was ground by #1000 emery paper, and then cleaned with ethanol and water in sequence. The C-ring specimen was stressed to 150 % of its room temperature yield strength (YS) at the apex using an Alloy 600 bolt and nut.

C	Mn	Si	P	S	Ni	Cr	Ti	Al	Co	Cu	Fe
0.024	0.23	0.13	0.005	<0.001	74.90	15.37	0.28	0.20	0.016	0.009	8.84

Table 1. Chemical composition of the Alloy 600 materials (wt%)

2.2 Electrochemical noise measurements

Fig. 1 is a schematic of the C-ring test facility and the EN experiments (Kim & Kim, 2009). The EN measurements were carried out with a Zahner IM6e equipped with a Zahner NProbe. In the PCCN mode, only ECN was recorded between the stressed and unstressed specimens during applying an anodic potential of 100 mV vs. open circuit potential (OCP). No information about the EPN was obtained in the PCCN mode. On the other hand, in the UCPN mode, the EPN of the stressed specimen were recorded relative to a reference electrode simultaneously with the ECN between the stressed and unstressed specimens at OCP.

The reference electrode was an external Ag/AgCl/KCl (0.1 M) electrode, specially designed and constructed for high temperature and pressure applications (Toshin-Kogyo Co., UH type). For reliable measurements of the electrochemical potential, the reference electrode was reassembled and recalibrated frequently during the interruption of the test series. The sample interval and the frequency bandwidth were 0.5 s and 1 mHz ~ 1 Hz, respectively. The power spectral density and the frequency of events were calculated from each set of time records that consisted of 2,048 data points acquired for 1×10^3 s.

2.3 C-ring immersion tests

In the PCCN mode, the test environment was an aqueous solution of 40 wt% NaOH containing 0.01 wt% PbO (leaded caustic solution). Pb-assisted SCC was accelerated by the potentiostatic method by maintaining the electrochemical potential in the active-passive range for Alloy 600 in caustic environments (Kim. et al., 2005). The C-ring tests in the PCCN mode were performed at 315 °C for 110 h.

In the UCPN mode, the tests were carried out in the leaded caustic solution, and that solution plus 500 ppm CuO. CuO was added to the leaded caustic solution to accelerate Pb-assisted SCC because CuO is a well-known oxidizing species that increases the corrosion potential and promotes Pb-assisted SCC (Jacko, 1990; Kim. et al., 2005). The C-ring tests in UCPN mode were performed at 290 °C for a total accumulated immersion time of 400 h, and

consisted of two phases of immersions in sequence; (a) 278 h in the leaded caustic solution (40 wt% NaOH with 0.01 wt% Pb) and (b) 122 h in that solution plus 500 ppm CuO. The addition of CuO caused an increase of the electrochemical potential by about 150 mV. The surfaces of the specimens were intermittently examined for cracking using an optical stereo-microscopy and scanning electron microscopy (SEM, JEOL JSM-6360).

Prior to the immersion test, the test solution was deaerated with 99.99 % nitrogen gas for 20 h. After the entire immersion test, the specimens were chemically etched with a solution of 2% bromine + 98% methanol, and then examined by SEM equipped with an energy dispersive spectrometer (EDS, Oxford-7582).
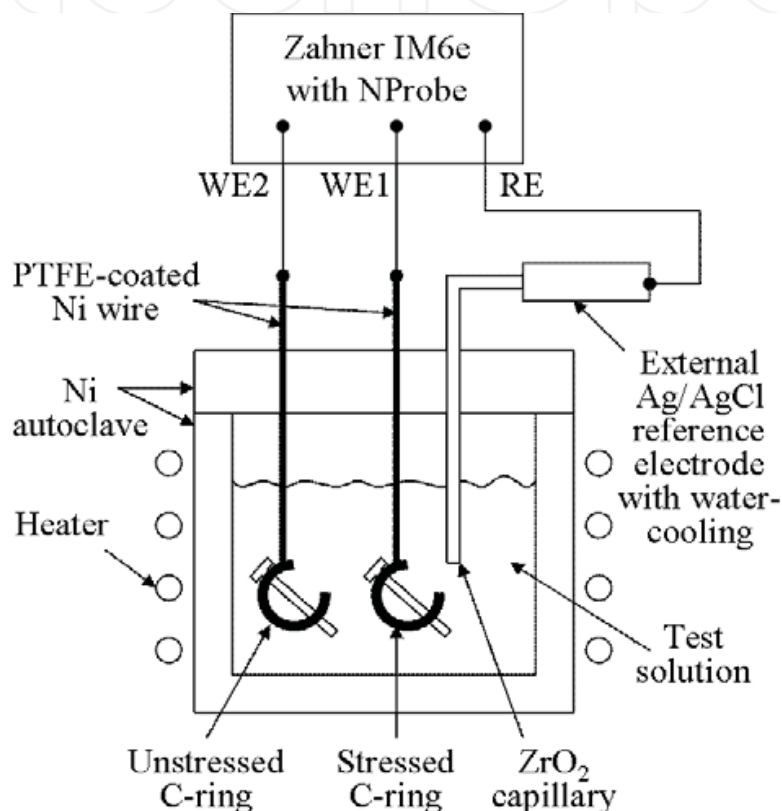
Fig. 1. Schematic of the C-ring test system and the electrochemical noise experiment

3. Results and discussion

3.1 Spectral analysis of electrochemical noise in PCCN mode

Fig. 2 gives the time record of the ECN measured from the stressed C-ring specimen in the leaded caustic solution at 315 °C for 110 h by the EN technique in the PCCN mode. There were abrupt changes in the ECN after immersion for 132×10^3 s (points B, C, D and E in Fig. 2), which have generally been observed during localized corrosions such as pitting corrosion, crevice corrosion, intergranular corrosion and SCC (Al-Mazeedi & Cottis, 2004; Cottis, 2001; Cottis et al., 2001; Kim & Kim, 2009; Sanchez-Amyay et al., 2005; Stewart et al., 1992). As compared with the ECN at point A, the ECN revealed repetitive current rises followed by fast decay with certain time interval in the time record at points B and C (see the insert in Fig. 2). This means that discrete events of a localized corrosion are occurring

from 132×10^3 to 158×10^3 s during the immersion in the leaded caustic solution. On the other hand, from 185×10^3 to 240×10^3 s, the ECN revealed current increases followed by slower decay with longer time interval in the time record at points D and E, indicating the occurrence of a localized corrosion event inducing larger charge passage than that at points B and C.

In order to correlate the changes of the ECN with the cracking stages, the test was interrupted and the surface of the specimen was examined for cracking at accumulated immersion times of 22, 42 and 110 h. After the immersion test in the leaded caustic solution for 22 h, the extensive examination of the surface of the specimen ruled out any cracking. At the accumulated immersion time of 42 h, it turned out that there were many defect sites such as local break-down of the surface oxide film and micro-cracks initiated with depth of one grain boundary or less in the OD surface from the SEM analysis of the C-ring apex as shown in Fig. 3(a). After the entire immersion test for 110 h, one of micro-cracks was propagated as presented in Fig. 3(b). The crack was propagated in an intergranular (IG) mode and the crack mouth and tip were covered by a surface oxide film, which is typical of SCC of Alloy 600 in leaded caustic environments (Hwang et al., 1997; Hwang et al., 1999; Kim et al., 2007; Kim et al., 2008). The chemical composition of the surface film was analyzed with EDS, and summarized in Table 2, along with the chemical composition of the Alloy 600 matrix.
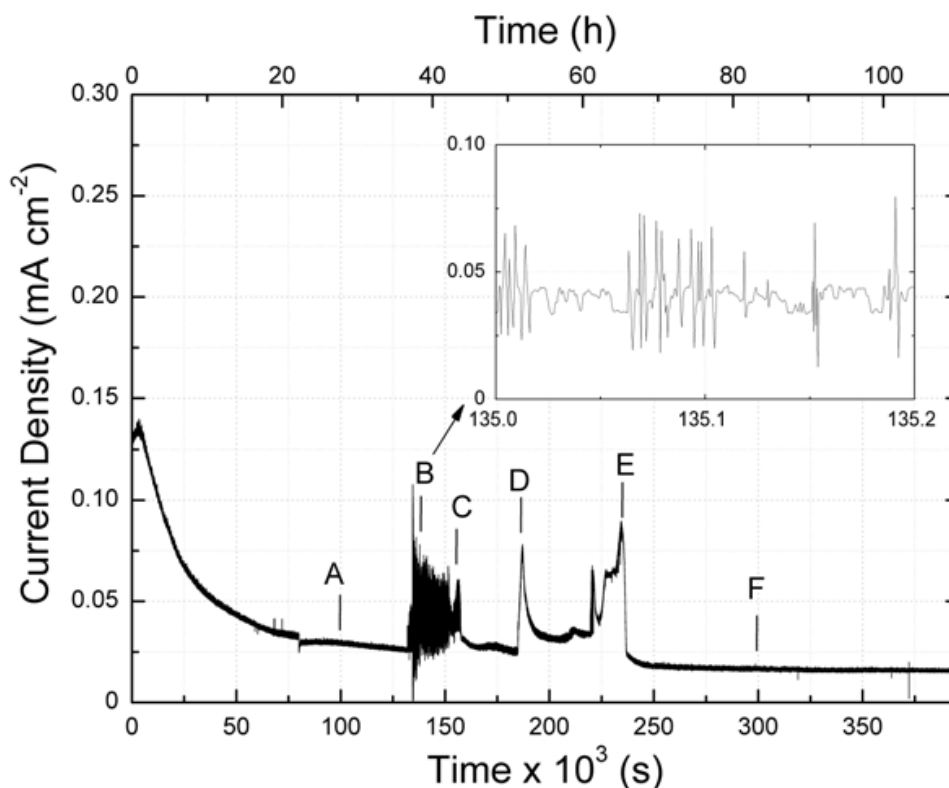

Fig. 2. Time records of the ECN measured in the PCCN mode from the stressed C-ring specimens in a 40 wt% NaOH solution containing 0.01 wt% PbO at 315 °C for 110 h. The test was interrupted and the specimen surface was examined for cracking at accumulated immersion times of 22, 42 and 110 h
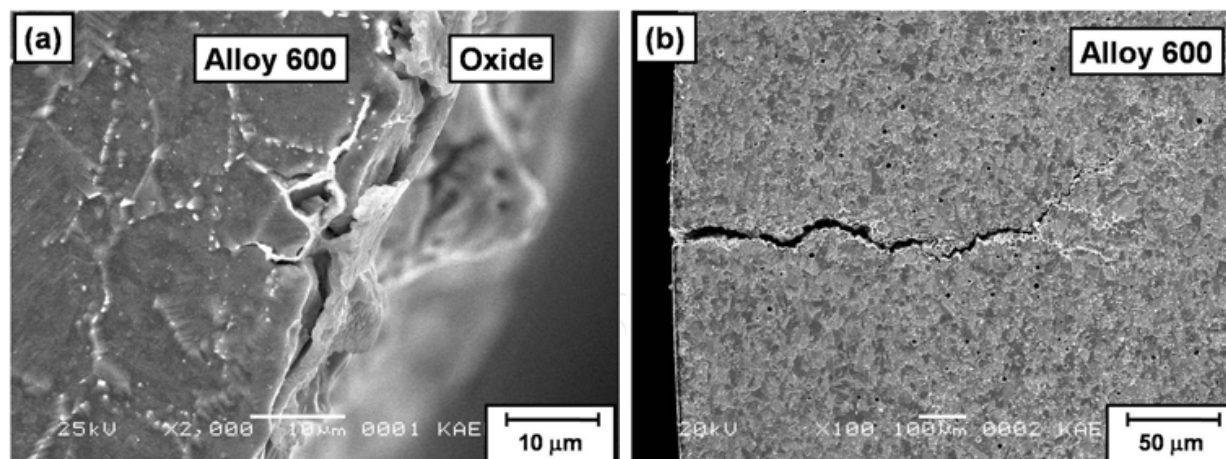
Fig. 3. SEM micrographs of the side surface of the C-ring apex after the accumulated immersion times of (a) 42 h and (b) 110 h in the leaded caustic solution at 315 °C

Position	O	Al	Ti	Cr	Mn	Fe	Ni
Matrix	ND*	0.31	0.18	15.74	0.27	8.35	75.14
Crack mouth	21.61	0.34	0.11	5.96	0.15	2.65	69.18
Crack tip	22.04	0.21	0.15	8.88	0.05	4.10	64.57

* ND : not detectable

Table 2. Chemical composition of the matrix and the surface film of the crack mouth and tip after a whole immersion test in 40 wt% NaOH solution containing 0.01 wt% PbO at 315 °C for 110 h (wt%)

With the aid of the microscopic analysis, it is easily anticipated that the current rises followed by steeper decay with shorter time interval in the time record of the ECN at points B and C in Fig. 2 are mainly due to the initiation of SCC, whereas the current increases followed by slower decay with longer time interval in the time record at points D and E in Fig. 2 are attributable to its propagation.

Figs. 4(a) and (b) present the plots of the power spectral density (PSD) vs. the frequency calculated from each time record of the ECN by a fast Fourier transform (FFT) algorithm at points A, B and C, and D, E and F, respectively. In Fig. 4(a), it is clearly seen that the PSD of the ECN obtained at points B and C where the initiation of SCC is expected to occur, is higher at whole frequency ranges than that obtained at point A where the general corrosion (the formation of the passive oxide film) occurs on the C-ring surface. Similar behaviors were found in Fig. 4(b), that is, the PSD of the ECN obtained at points D and E where the propagation of SCC is supposed to occur, is higher than that obtained at point F, except the remarkable increase of the PSD at a low frequency limit. The increases of the PSD especially at a low frequency limit in Figs. 4(a) and (b) strongly indicates the increase in the number of localized corrosion events, that is, the initiation and the propagation of Pb-assisted SCC, respectively, as previously reported (Kim & Kim et al., 2009a; Kim & Kim et al., 2009b). Since the type of corrosion can not be reliably distinguished on the basis of the roll-off slope (Cottis, 2001), it will not be considered as indicator of localized corrosions in this work.
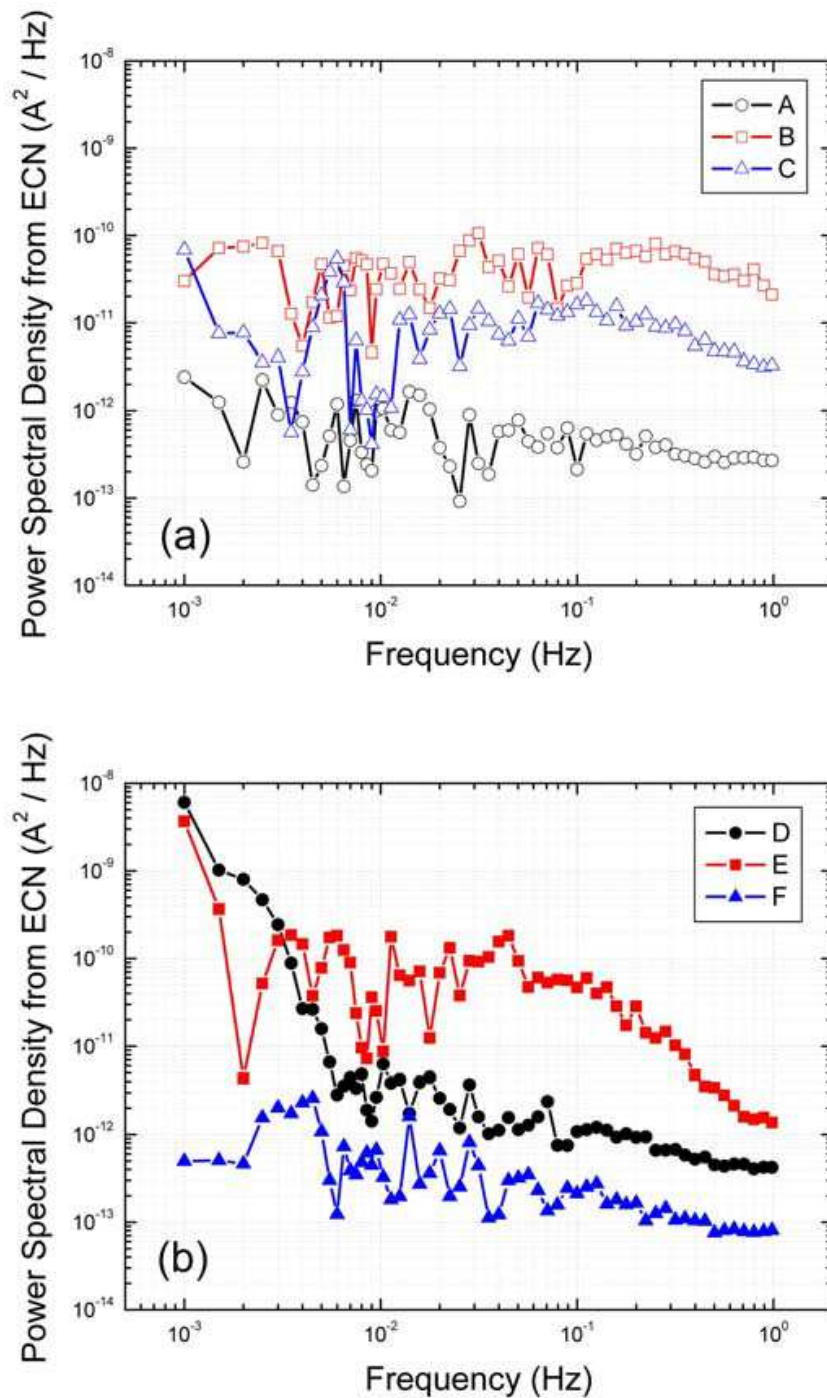
Fig. 4. Plots of the PSD vs. the frequency calculated from each time record of the ECN by the FFT algorithm at points (a) A, B and C, and (b) D, E and F

3.2 Spectral analysis of electrochemical noise in UCPN mode

Figs. 5(a) and (b) give typical EPN and ECN recorded from the stressed specimen in the leaded caustic solution for the time period from 982×10^3 to 996×10^3 s, and for that solution plus CuO for the time period from 1406×10^3 to 1420×10^3 s, respectively, by the EN measurement in the UCPN mode. There were typical current increases in the ECN concurrent with the potential drops in the EPN at points A, C, D and F, which have also

generally been observed during localized corrosions; the current increase corresponding to the potential decrease means a local break-down of the oxide film resulting in an exposure and local dissolution of the metal surface, whereas the current decrease accompanied by the potential recovery indicates a repair of the surface oxide film (repassivation).
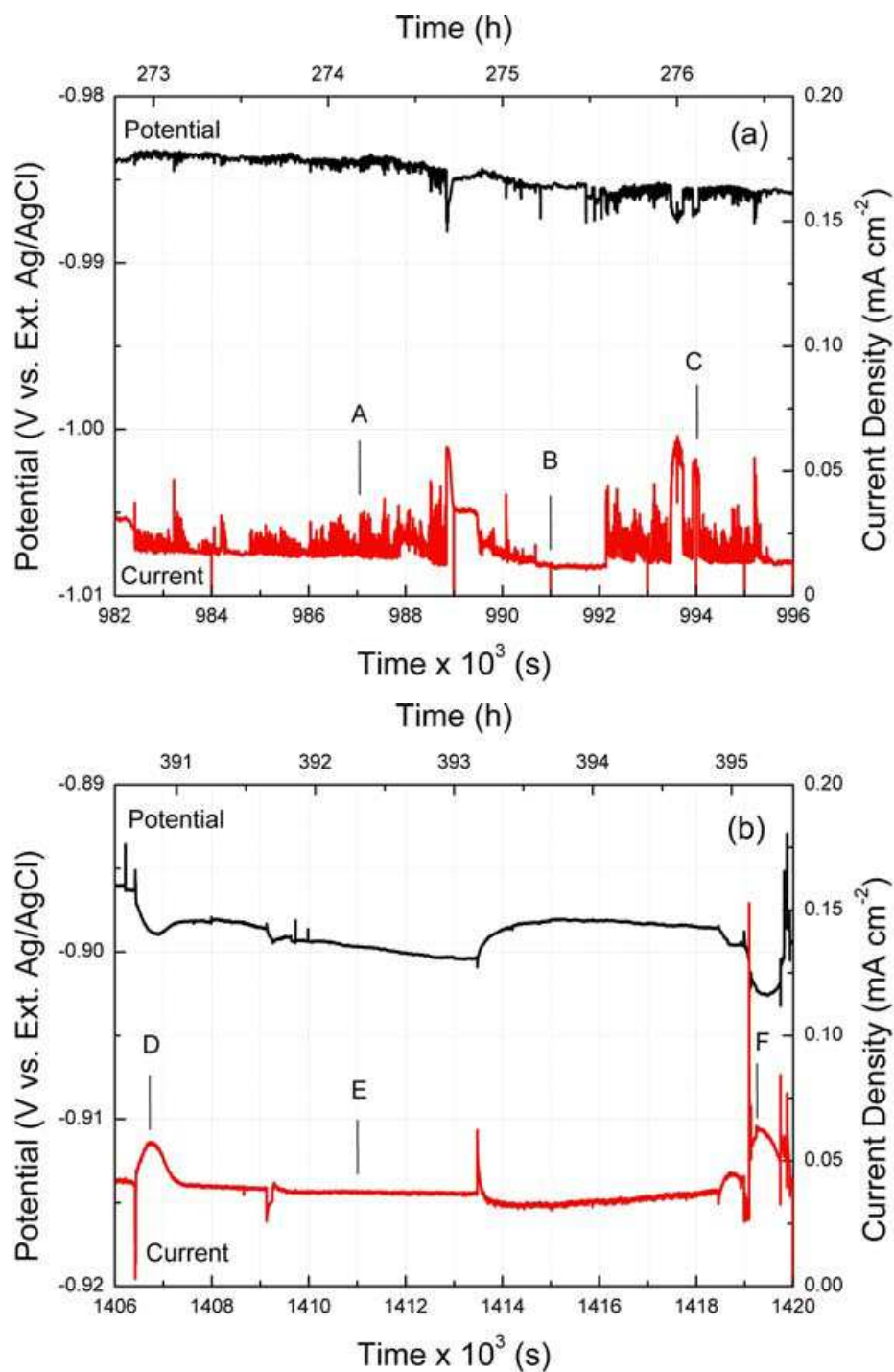

Fig. 5. Time records of the EPN and the ECN recorded in UCPN mode (a) for the leaded caustic solution for the time period from 980×10^3 to 996×10^3 s, and (b) for that solution plus CuO for the time period from 1405×10^3 to 1421×10^3 s at 290 oC

The ECN at points A and C in Fig. 5(a) revealed repetitive current increases followed by faster decay with shorter time interval when compared to the ECN at points D and F in Fig. 5(b) exhibiting more localized behavior, that is, current rises followed by slower decay with longer time interval. It is notable that the behavior of the ECN at points A and C recorded in the UCPN mode (Fig. 5(a)) was fairly similar with that of the ECN at points B and C obtained in the PCCN mode (Fig. 2). Also, the ECN at points D and F in the UCPN mode (Fig. 5(b)) resembles the ECN at points D and E in the PCCN mode (Fig. 2) in appearance.

After the immersion test in the leaded caustic solution for 278 h, the surface of the specimen was extensively examined for cracking. From the SEM analysis, the local break-down of the surface oxide film and many defect sites were found on the surface of the stressed specimen (Fig. 6(a)). After the entire immersion test in the leaded caustic solution plus CuO for 400 h, several cracks were propagated in the IG mode (Fig. 6(b)). Consequently, it is strongly suggested that the current increases in the ECN accompanied by the potential drops in the EPN in Fig. 5(a) are mainly due to the initiation of SCC and those changes in the ECN and the EPN in Fig. 5(b) are attributable to its propagation.

Figs. 7(a) and (b) present the plots of the PSD vs. the frequency calculated from each time record of the ECN and the EPN, respectively, by the FFT algorithm at points A, B and C in Fig. 5(a). It is obvious that the PSD of both ECN and EPN at points A and C, where SCC is expected to be initiated in the leaded caustic solution, is higher at whole frequency ranges than that obtained at point B where the general corrosion (the repassivation of the surface oxide film) occurs on the C-ring surface. Similar trends were observed in Figs. 8(a) and (b); the PSD of ECN and EPN at points D and F, where SCC is supposed to be propagated in the leaded caustic solution plus CuO, is higher than that obtained at point E. It is noticeable that the PSD of both ECN and EPN due to the propagation of SCC (Figs. 8(a) and (b)) revealed more dominant increase at a low frequency limit as compared to that PSD due to the initiation of SCC (Figs. 7(a) and (b)), indicating more localized characteristics of the propagation of SCC. The results from the spectral analyses of the ECN and the EPN recorded in the UCPN mode are well coincided with that obtained in the PCCN mode.
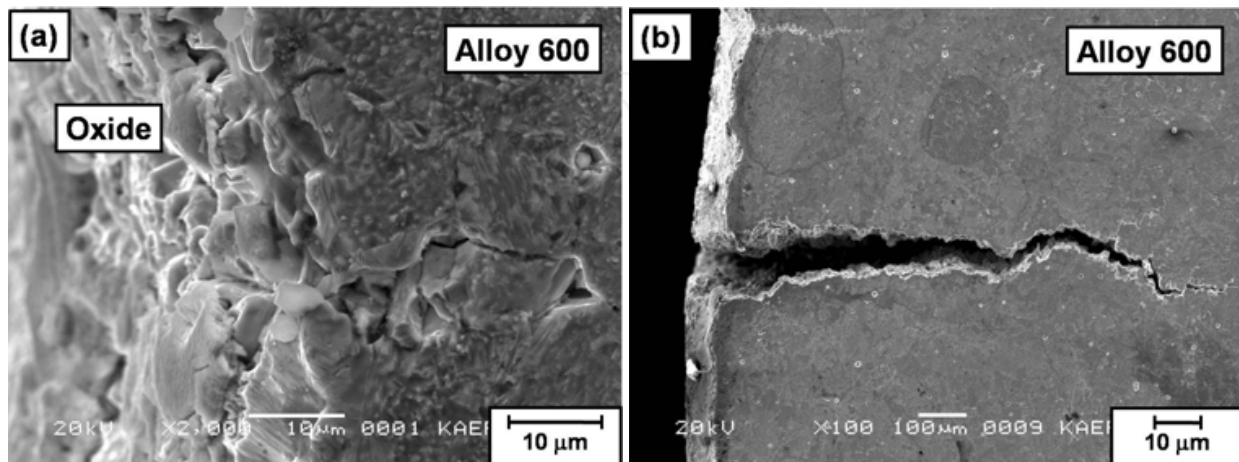

Fig. 6. SEM micrographs of the side surface of the C-ring apex after the accumulated immersion times of (a) 278 h in the leaded caustic solution and (b) 400 h in that solution plus CuO at 290 ºC
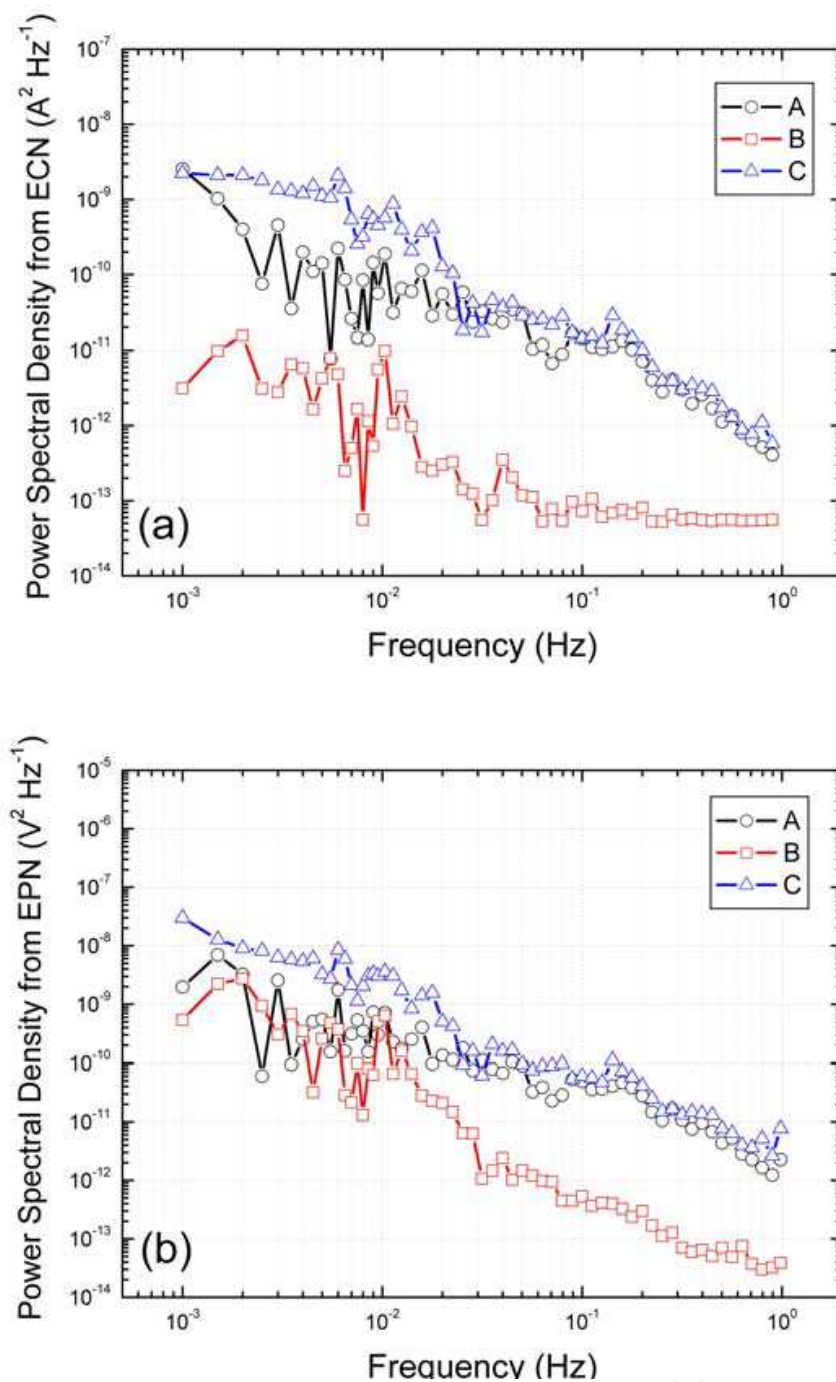
Fig. 7. Plots of the PSD vs. the frequency calculated from each time record of (a) the ECN and (b) the EPN by the FFT algorithm at points A, B and C in Fig. 5(a)

3.3 Stochastic analysis of electrochemical noise

To evaluate the stochastic characteristics of the initiation and the propagation of SCC, a shot-noise analysis was employed in this work under the assumption that the ECN concurrent with the EPN is independently produced by the individual event of localized corrosions. Based on the shot-noise theory (Al-Mazeedi & Cottis, 2004; Cottis, 2001; Sanchez-Amyay et al., 2005), the frequency of events f_n of the localized corrosions is determined from the time record of the EPN as given by,

$$f_n = B^2/(\Psi_E A) \tag{1}$$

where B is the Stern-Geary coefficient, Ψ_E the PSD value of the EPN calculated by averaging several low-frequency points using the FFT algorithm and A represents the exposed electrode area.
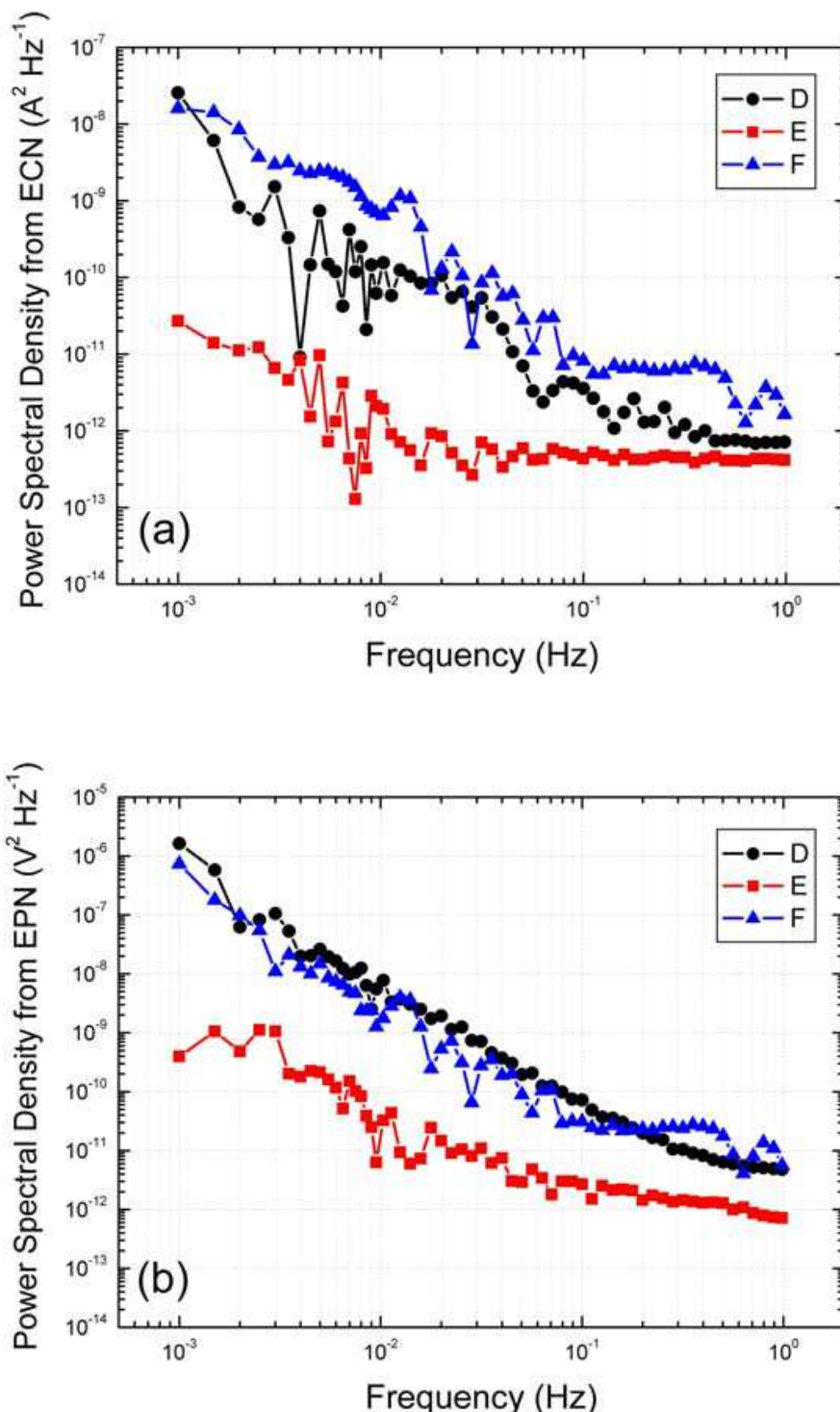

Fig. 8. Plots of the PSD vs. the frequency calculated from each time record of (a) the ECN and (b) the EPN by the FFT algorithm at points D, E and F in Fig. 5(b)

From a set of f_n calculated from the PSD plots of the EPN according to Eq. (1), the cumulative probability $F(f_n)$ at each f_n is determined numerically by a mean rank approximation (Cottis, 2001). In this work, the probability of f_n for the Pb-assisted SCC was analyzed using the Weibull distribution function, the most commonly used cumulative probability function for predicting a life and failure rate (Na & Pyun, 2007; Na et al., 2007a; Na et al., 2007b). Using the Weibull distribution function, the probability of the mean time-to-failure, t_n, which corresponds to $1/f_n$, is expressed as,

$$\ln\{\ln[1/(1-F(t_n))]\} = m \ln t_n - \ln n \qquad (2)$$

where m and n are the shape and scale parameters, respectively.

Fig. 9 demonstrates the plots of $\ln\{\ln[1/(1-F(t_n))]\}$ vs. $\ln t_n$ calculated from the sets of f_n at the same time period as Figs. 5(a) and (b). For a comparison, the probability of t_n obtained from the EN measurement of two identical unstressed Alloy 600 specimens in a 40 wt% NaOH solution without impurities at 290 ºC is also plotted. Only general corrosion occurred on the unstressed specimen surface without any cracking. In Fig. 9, it was easily anticipated that the mean time-to-failure t_n for the localized corrosions such as the initiation and the propagation of SCC shifted to a higher value, analogous to the shift of f_n to a lower frequency when compared to that for the general corrosion.
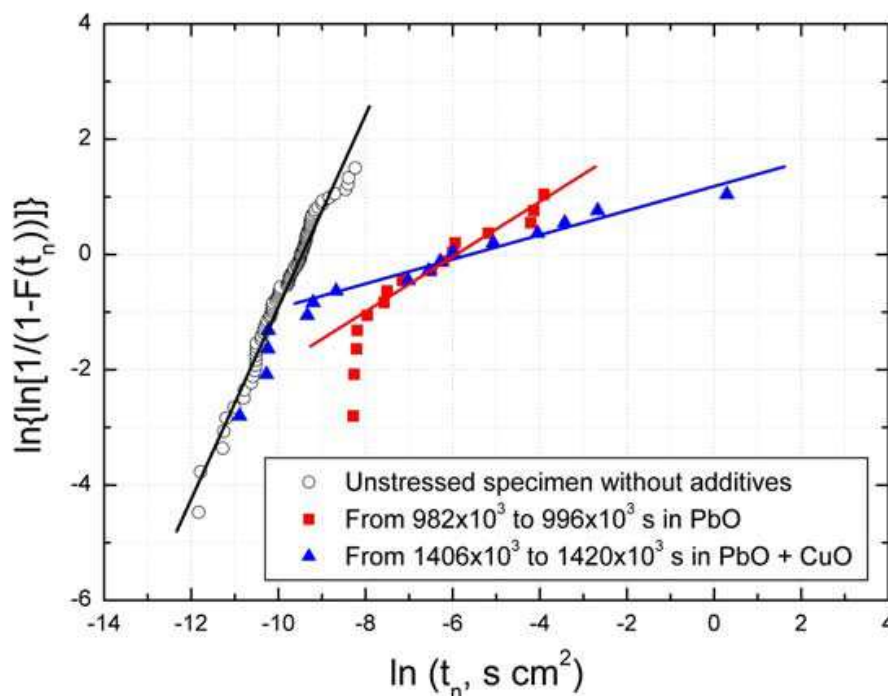

Fig. 9. Plots of $\ln\{\ln[1/(1-F(t_n))]\}$ vs. $\ln t_n$ calculated from the sets of fn at the same time period as Figs. 5(a) and (b). For a comparison, the probability of t_n obtained from the EN measurement of two identical unstressed Alloy 600 specimens in a 40 wt% NaOH solution without impurities at 290 ºC is also plotted

In previous works (Na & Pyun, 2007; Na et al., 2007a; Na et al., 2007b; Park & Pyun, 2004; Pyun et al., 1993; Pyun et al., 1994), the conditional event generation rate $r(t)$ of a localized corrosion was introduced as a failure rate using the values of m and n as,

$$r(t) = (m/n) \, t^{m-1} \tag{3}$$

Depending on the corrosion mechanism, the value of r(t) was regarded as the rate of localized corrosion events such as the pit generation (Pyun et al., 1994), the pit growth (Park & Pyun, 2004) and the propagation of SCC (Na et al., 2007b). There are few reports on the stochastic approach for the localized corrosions of Alloy 600 materials at high temperature in the literature. For stainless steels, Shibata (Shibata, 1990; Shibata, 2007) reviewed the stochastic studies on a passive film break-down triggering the initiation of localized corrosions. He analysed the stochastic characteristics of the local break-down and the repair of the passive film using the Poisson stochastic theory by assuming a completely random occurrence. For the Poisson process, the value of m in the Weibull probability is unity. In a real situation, however, there is a distortion in the Poisson probability, and hence, a deviation of the value of m from unity, caused by a difference in many experimental conditions such as the chemistry of the test solution, the applied potential and the interactions between localized events.

On the other hand, Pyun et al. reported that the value of m increases from 0.7 up to unity with a decreasing applied potential (Pyun et al., 1993) for the pit generation at the surface of Al alloy at room temperature, and the value of m decreases from 0.4 to 0.1 with the addition of SO_4^{2-} and MoO_4^{2-} ions in a 0.1 M NaCl solution (Na et al., 2007a) and with the addition of SO_4^{2-}, NO_3^{-} and PO_4^{3-} ions in a 1M HCl solution (Na & Pyun, 2007) for the pit initiation at the surface of pure Al at room temperature. Interestingly, they also reported that the value of m is 0.33 for the SCC propagation of Alloy 600 in a neutral solution containing PbO at room temperature (Na et al., 2007b).

In our previous works (Kim & Kim, 2009a; Na et al., 2007a; Na et al., 2007b), it was reported that the shape parameter m of the Weibull distribution can be regarded as an indicator of types of corrosion. In the present work, the value of m determined from Fig. 9 by a linear curve fitting method were 1.46 for the general corrosion on the unstressed specimen in the caustic solution without any oxidizing impurities, 0.47 for the initiation of SCC on the stressed specimen in the leaded caustic solution, and 0.21 for its propagation in the leaded caustic solution plus CuO. The values of m in this work revealed good agreement with those values previous reported for each stage of the Pb-assisted SCC (Kim & Kim, 2009a).

4. Conclusions

From the microscopic and the EN analyses of Alloy 600 SG tube materials in the leaded caustic solution environment at high temperature, it is strongly suggested that the repetitive current rises followed by steeper decay with shorter time interval in the time record of the ECN measured in the PCCN mode are mainly due to the initiation of SCC, whereas the current increases followed by slower decay with longer time interval are attributable to its propagation.

From the spectral analysis of the ECN, the PSD increased more remarkably at low frequency limit for the propagation of SCC as compared to that for the initiation of SCC. Similar trends were observed in both ECN and EPN measured in the UCPN mode in the caustic solution environments with various oxidizing impurities. In addition, from the stochastic analysis of the EPN obtained in the UCPN mode, it was found the shape parameter of the Weibull distribution of the mean time-to-failure for the initiation of SCC is clearly distinguishable from that parameter for the propagation of SCC as well as for the general corrosion.

5. Acknowledgement

6. References

Al-Mazeedi, H.A.A. & Cottis, R.A. (2004). A practical evaluation of electrochemical noise parameters as indicators of corrosion type, *Electrochim. Acta*, Vol. 49, p. 2787

Cottis, R.A. (2001). Interpretation of electrochemical noise data, *Corrosion*, Vol. 57, p. 265

Cottis, R.A. ; Al-Awadhi, M.A.A.; Al-Mazeedi H. & Turgoose, S. (2001). Measures for the detection of localized corrosion with electrochemical noise, *Electrochim. Acta*, Vol. 46, p. 3665

Hwang, S.S.; Kim, U.C & Park, Y .S. (1997). The effects of Pb on the passive film of Ni-base alloy in high temperature water, *J. Nucl. Mater.*, Vol. 246, p. 77

Hwang, S.S. ; Kim, H.P.; Lee, D.H.; Kim, U.C & Kim, J.S. (1999). The mode of stress corrosion cracking in Ni-base alloys in high temperature water containing lead, *J. Nucl. Mater.*, Vol. 275, p. 28

Jacko, R.J. (1990). *Corrosion Evaluation of Thermally Treated Alloy 600 Tubing in Primary and Faulted Secondary Water Environments*, EPRI NP-6721, Pittsburgh, Pennsylvania

Kim, D.J. Kim; Kwon, H.C & Kim, H.P. (2008). Effects of the solution temperature and the pH on the electrochemical properties of the surface oxide films formed on Alloy 600, *Corros. Sci.*, Vol. 50, p. 1221

Kim, H.P.; Hwang, S.S.; Kim, J.S. & Hwang, J.H. (2007). Stress corrosion cracking of steam generator tubing materials in lead containing solution, *Proc. of the 13th Int. Conf. on Environmental Degradation of Materials in Nuclear Power Systems*, Whistler, Canada, Aug. 19-23, 2007

Kim, S.W. & Kim, H.P. (2009a). Electrochemical noise analysis of PbSCC of Alloy 600 SG tube in caustic environments at high temperature, *Corros. Sci.*, Vol. 51, p. 191

Kim, S.W. & Kim, H.P. (2009b). Interpretation of electrochemical noise parameters as indicators of initiation and propagation of SCC of an Alloy 600 SG tube at high temperatures, *Nuclear Enginnering and Technology*, Vol. 41, p. 1315

Kim, U.C.; Kim, K.M. & Lee, E.H. (2005). Effects of chemical compounds on the stress corrosion cracking of steam generator tubing materials in a caustic solution, *J. Nucl. Mater.*, Vol. 341, p. 169

Na, K.H. & Pyun, S.I. (2007). Effects of sulphate, nitrate and phosphate on pit initiation of pure aluminium in HCl-based solution, *Corros. Sci.*, Vol. 49, p. 2663

Na, K.H.; Pyun, S.I. & Kim, H.P. (2007a). Analysis of electrochemical noise obtained from pure aluminium in neutral chloride and alkaline solutions, *Corros. Sci.*, Vol. 49, p. 220

Na, K.H.; Pyun, S.I. & Kim, H.P. (2007b). Effects of NiB, PbO, and TiO_2 on SCC of sensitized Inconel Alloy 600 in RT-tetrathionate solution, *J. Electrochem. Soc.*, Vol. 154, p. C349

Park, J.J. & Pyun, S.I. (2004). Stochastic approach to the pit growth kinetics of Inconel alloy 600 in Cl⁻ ion-containing thiosulphate solution at temperatures 25-150 ₒC by analysis of the potentiostatic current transients, *Corros. Sci.*, Vol. 46, p. 285

Pyun, S.I.; Lee, E.J. & Kim, C.H. (1993). Stochastic approach to analysis of pitting corrosion of anoidc oxide film on Al-1wt.%Si-0.5wt.%Cu alloy, *Surf. Coat. Tech.*, Vol. 62, p. 480

Pyun, S.I.; Lee, E.J. & Han, G.S. (1994). Localized corrosion of sputtered Al-1wt.%Si-0.5wt.%Cu alloy thin film, *Thin Solid Films*, Vol. 239, p. 74

Sakai,T.; Okabayashi, S.; Aoki, K.; Matsumoto, K. & Kishi, Y. (1990). A study of oxide thin film of Alloy 600 in high temperature water containing lead, *Corrosion/90*, paper no. 520, NACE, Houston

Sanchez-Amyay, J.M.; Cottis, R.A. & Botana, F.J. (2005) Shot noise and statistical parameters for the estimation of corrosion mechanisms, *Corros. Sci.*, Vol. 47, p. 3280

Shibata, T. (1990). Stochastic studies of passivity breakdown, *Corros. Sci.*, Vol. 31, p. 413

Shibata, T. (2007). Passivity breakdown and stress corrosion cracking of stainless steel, *Corros. Sci.*, Vol. 49, p. 20

Stewart, J.; Wells, D.B.; Scott, P.M. & Williams, D. E. (1992). Electrochemical noise measurements of stress corrosion cracking of sensitised austenitic stainless steel in high-purity oxygenated water at 288 ºC, *Corros. Sci.*, Vol. 33, p. 73
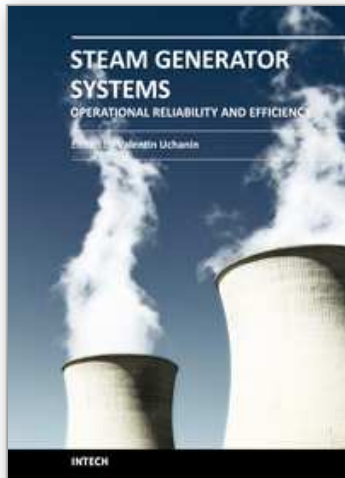
Steam Generator Systems: Operational Reliability and Efficiency

Edited by Dr. Valentin Uchanin

The book is intended for practical engineers, researchers, students and other people dealing with the reviewed problems. We hope that the presented book will be beneficial to all readers and initiate further inquiry and development with aspiration for better future. The authors from different countries all over the world (Germany, France, Italy, Japan, Slovenia, Indonesia, Belgium, Romania, Lithuania, Russia, Spain, Sweden, Korea and Ukraine) prepared chapters for this book. Such a broad geography indicates a high significance of considered subjects.

How to reference

In order to correctly reference this scholarly work, feel free to copy and paste the following:

Sung-Woo Kim, Hong-Pyo Kim, Seong-Sik Hwang and Dong-Jin Kim (2011). In-situ Monitoring of SCC of Alloy 600 SG Tubing in PWR using EN Analysis, Steam Generator Systems: Operational Reliability and Efficiency, Dr. Valentin Uchanin (Ed.), ISBN: 978-953-307-303-3, InTech, Available from: http://www.intechopen.com/books/steam-generator-systems-operational-reliability-and-efficiency/in-situ-monitoring-of-scc-of-alloy-600-sg-tubing-in-pwr-using-en-analysis

INTECH
open science | open minds